Science of the Total Environment 829 (2022) 154642

Contents lists available at ScienceDirect

Science of the Total Environment

journal homepage: www.elsevier.com/locate/scitotenv

Influence of strong iron-binding ligands on cloud water oxidant capacity

Aridane G. González [a,b,*], Angelica Bianco [c,*], Julia Boutorh [b], Marie Cheize [b], Gilles Mailhot [d], Anne-Marie Delort [d], Hélène Planquette [b], Nadine Chaumerliac [c], Laurent Deguillaume [c,e], Geraldine Sarthou [b]

[a] Instituto de Oceanografía y Cambio Global, IOCAG, Universidad de Las Palmas de Gran Canaria, ULPGC, Spain
[b] CNRS, Univ Brest, IRD, Ifremer, LEMAR, F-29280 Plouzane, France
[c] Laboratoire de Météorologie Physique, UMR 6016, CNRS, Université Clermont Auvergne, 63178 Aubière, France
[d] CNRS, SIGMA Clermont, Institut de Chimie de Clermont-Ferrand, Université Clermont Auvergne, F-63000 Clermont-Ferrand, France
[e] Observatoire de Physique du Globe de Clermont-Ferrand, UAR 833, CNRS, Université Clermont Auvergne, 63178 Aubière, France

HIGHLIGHTS

- 95% of iron is complexed by strong organic ligands, likely produced by microorganisms.
- Fe complexes stability constants are much higher than those used in cloud chemistry.
- The presence of strong organic ligands induces an increase in hydroxyl radical production.
- The analysis of sources and sinks of •OH highlighted that complexed iron does not deplete $HO_{2/O2^-}$•.

GRAPHICAL ABSTRACT

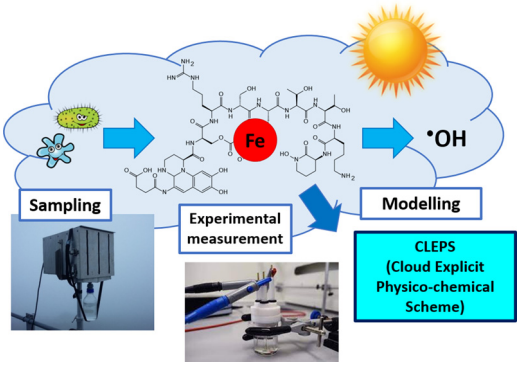

ARTICLE INFO

Article history:
Received 1 December 2021
Received in revised form 9 March 2022
Accepted 14 March 2022
Available online 17 March 2022

Editor: Pingqing Fu

Keywords:
Cloud oxidant capacity
Iron complexation
Cloud chemistry modelling
Cloud microbiota

ABSTRACT

Iron (Fe) plays a dual role in atmospheric chemistry: it is involved in chemical and photochemical reactivity and serves as a micronutrient for microorganisms that have recently been shown to produce strong organic ligands. These ligands control the reactivity, mobility, solubility and speciation of Fe, which have a potential impact on Fe bioavailability and cloud water oxidant capacity.

In this work, the concentrations of Fe-binding ligands and the conditional stability constants were experimentally measured for the first time by Competitive Ligand Exchange-Adsorptive Cathodic Stripping Voltammetry (CLE-ACSV) technique in cloud water samples collected at puy de Dôme (France). The conditional stability constants, which indicate the strength of the Fe-ligand complexes, are higher than those considered until now in cloud chemistry (mainly Fe-oxalate). To understand the effect of Fe complexation on cloud water reactivity, we used the CLEPS cloud chemistry model. According to the model results, we found that Fe complexation impacts the hydroxyl radical formation rate: contrary to our expectations, Fe complexation by natural organic ligands led to an increase in hydroxyl radical production. These findings have important impacts on cloud chemistry and the global iron cycle.

* Correspondence to: A. Bianco, Laboratoire de Météorologie Physique, UMR 6016, CNRS, Université Clermont Auvergne, 63178 Aubière, France, and A. G. Gonzales, CNRS, Univ Brest, IRD, Ifremer, LEMAR, F-29280 Plouzane, France.
E-mail addresses: aridane.gonzalez@ulpgc.es (A.G. González), angelica.bianco@uca.fr (A. Bianco).

http://dx.doi.org/10.1016/j.scitotenv.2022.154642

1. Introduction

Determining the concentrations of trace elements and their speciation in cloud water is of ecological interest because atmospheric deposition is one of the main nutrient sources for nutrient-poor environments. Iron (Fe) is particularly important in this context since it is essential for photosynthesis and is the limiting element for phytoplankton growth in most oceanic regions (Buesseler et al., 2008). Fe is present in atmospheric waters at concentrations that vary from ng to μg L^{-1}; this Fe partly results from the dissolution of atmospheric aerosols (Deguillaume et al., 2005). The Fe solubility is accelerated when the acidity increases, but the nature of the solid matrix and photochemistry govern the kinetics of dissolution (Tapparo et al., 2020; Sherman, 2005). In atmospheric water, Fe can be trapped in crystalline inorganic structures such as dust particles and thus, it is not bioavailable for microorganisms. Fe can also be present as soluble complexes, which can easily enter the microbial metabolism.

In cloud water, Fe is mainly found in two oxidation states: Fe(II) and Fe(III). Acidity, redox potential (Bianco et al., 2020) and organic compounds govern Fe(III) reactivity, mobility, solubility and speciation in natural waters (Deguillaume et al., 2005; Liu and Millero, 2002; Passananti et al., 2016; Gledhill and Buck, 2012a). In addition, photochemistry controls the Fe redox chemistry through Fenton and photo-Fenton cycles (Willey et al., 2000; Sigg et al., 2001; Deutsch et al., 2001; Warneck, 2000). Recent studies have demonstrated the viability of microorganisms and their metabolic activity in cloud waters (Skidmore et al., 2000; Toom-Sauntry and Barrie, 2002; Amato et al., 2007), enabling them to produce siderophores, which are ligands with high affinity for Fe (Vinatier et al., 2016; Amato et al., 2019).

Until now, oxalate has been commonly considered in cloud chemistry models as the dominant organic ligand of Fe(III) because of its elevated conditional stability constant (K_{cond} = 9.4) (Tapparo et al., 2020; Herrmann, 2003). Other Fe-binding ligands, such as exopolymers, siderophores or humic substances, which have higher K_{cond} values, are not currently considered in cloud chemistry models because of the lack of experimental data about their concentrations and K_{cond}. In cloud waters, Fe(III)-organic complexation may affect the formation of photogenerated hydroxyl radicals, •OH (Bianco et al., 2015; Huang et al., 2012), because when Fe is trapped in a complex, its reactivity is modified. Cloud chemistry models usually overestimate the production of •OH by Fenton and photo-Fenton reactions when considering only Fe as aqua-complexes (Bianco et al., 2015). Consequently, stronger Fe-binding ligands must be considered to model realistic Fe speciation and more relevant cloud oxidant capacity (Herrmann et al., 2015; Herckes et al., 2013).

For the first time, we determined the Fe-binding ligand concentrations and K_{cond} in cloud waters sampled at the puy de Dôme station (PUY, France). This work is crucial for improving cloud chemistry models that simulate multiphasic cloud processes, considering the explicit chemistry of transition metal ions that controls the cloud oxidant capacity. In this work, the detailed cloud chemistry model CLEPS 1.1 (Cloud Explicit Physico-chemical Scheme) was completed by considering the real natural speciation of Fe to evaluate its effect on the cloud oxidant capacity. Discerning the equilibrium between species is therefore essential to understand the biogeochemical cycle of this element (Johnson and Meskhidze, 2013). Moreover, evaluating the different chemical forms of Fe is crucial since it plays a key role in chemical and photochemical cycles that drive cloud oxidant capacity (Deguillaume et al., 2005; Bianco et al., 2020).

2. Materials and methods

2.1. Classification of cloud water samples and air mass origin

Cloud water samples were collected at the top of puy de Dôme (45.7722°N, 2.9648°E; 1465 m a.s.l.) in the Massif Central region (France) within the framework of PUYCLOUD observation service (https://www.opgc.fr/data-center/public/data/puycloudd). The procedure is described in the Supplementary information (SI) Sections in SI-S1 and SI-S2. Six cloud events collected between 2013 and 2016 (Table 1 and Table S1) were studied in this work. Within this analytical context (Deguillaume et al., 2014; Renard et al., 2020), samples collected at PUY are classified into four categories: highly marine, marine, continental and polluted. Among the 6 cloud samples, two were identified as marine (CW2 and CW4), and four were identified as continental (CW1, CW3, CW5 and CW6). In addition, the back trajectories of air masses computed with the CAT model (Fig. S1) corroborate these origins (Baray et al., 2020). In general, the marine category showed lower concentrations of ions, than the continental and polluted categories, which showed higher concentrations of NH_4^+, NO_3^- and SO_4^{2-}. This classification is helpful for the analysis, since in a previous work, the •OH formation rate was shown to be correlated with the air mass origin. In particular, at PUY, Fe concentrations were lower for the marine class than for the continental one (Bianco et al., 2015).

2.2. Competitive Ligand Exchange-Adsorptive Cathodic Stripping Voltammetry (CLE-ACSV)

Fe-complexing capacity in cloud waters was characterised using Competitive Ligand Exchange-Adsorptive Cathodic Stripping Voltammetry (CLE-ACSV) (SI-S3 and S4). Fe-complexing capacity has been previously measured in seawater (Aldrich and van den Berg, 1998), lake waters (Nagai et al., 2007) and rainwaters (Cheize et al., 2012), as well as for single model ligands (González et al., 2019). This technique allows us to measure the concentrations of Fe-binding ligands and the conditional stability constants of the Fe complexes $K_{Cond,\ Fe^{3+}Lig}$, which enables the classification as strong L_1-type ligands ($\log K_{Cond,\ Fe^{3+}Lig} > 22$) or as weak ligands of L_2 and L_3-type ($\log K_{Cond,\ Fe^{3+}Lig}$ ~21–22 and <21, respectively) (Gledhill and Buck, 2012b). The experimental determination of this value allows for

Table 1
Chemical parameters and Fe speciation results measured for the different cloud water samples collected at PUY. TdFe refers to the Fe measured in the sample without filtration and acidified at pH < 2. Fe′ is the labile Fe (inorganic Fe(II) + Fe(III)). L_{Fe} is the concentration of Fe-binding ligands in solutions, log K_{cond} are expressed for the free iron (Fe^{3+}) and labile Fe (Fe′). The percentage of Fe complexed (Fe-L). DOC = dissolved organic carbon. NM = not measured.

	Cloud samples					
Samples	CW2	CW4	CW1	CW3	CW5	CW6
Category	Marine	Marine	Continental	Continental	Continental	Continental
pH	5.4	4.9	4.9	5.2	5.4	4.8
TdFe (nM)	47 ± 3	40 ± 6	115 ± 3	226 ± 9	323 ± 6	95 ± 5
Fe′ (nM)	1.58	1.87	0.91	10.75	0.89	[a]
Oxalate	8.2 ± 0.2	0.4 ± 0.1	3.2 ± 0.1	2.2 ± 0.1	2.6 ± 0.1	1.9 ± 0.1
L_{Fe} (nM)	97 ± 22	135 ± 75	215 ± 42	378 ± 25	430 ± 91	[a]
$\log K_{Cond,\ Fe^{3+}}$	21.8 ± 0.4	21.5 ± 0.4	22.3 ± 0.7	21.3 ± 0.4	22.7 ± 0.1	[a]
$\log K_{Cond,\ Fe'}$	8.6 ± 0.4	8.3 ± 0.4	9.1 ± 0.7	8.1 ± 0.4	9.5 ± 0.1	[a]
%Fe-L	96.7	95.4	99.2	95.2	99.7	[a]

[a] Saturation of organic ligands with Fe prevents the determination of L_{Fe} and other parameters for sample CW6.

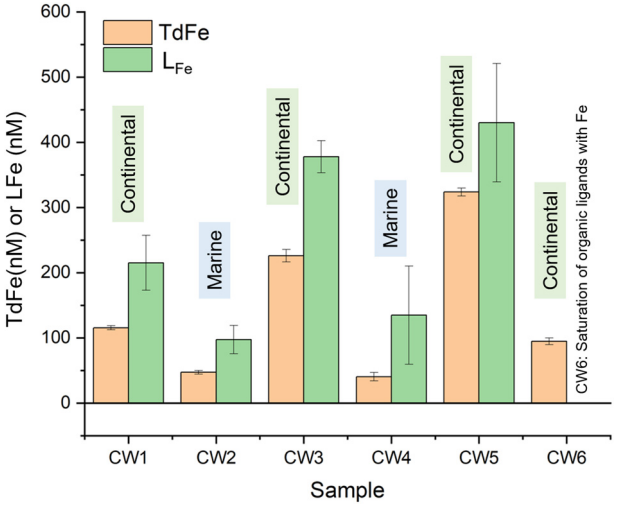

Fig. 1. TdFe concentrations (in orange) and natural Fe-binding ligands (L_{Fe}) (in green) in nM measured in the cloud water samples collected at PUY.

comparison with natural organic ligands, even if it does not provide any information about the chemical structure (Luther et al., 2001), and can be implemented into models to study Fe speciation.

TdFe, labile Fe (*Fe'*; is the sum of inorganic Fe(II) and Fe(III) species), Fe-binding ligands (L_{Fe}), $\log K_{Cond,\ Fe^{3+}Lig}$ for free Fe^{3+} and the percentage of Fe-organically complexed (%*FeL*) are reported in Table 1 and Fig. 1.

2.3. Modelling set-up

CLEPS 1.1 is a cloud chemistry model that enables the prediction of the aqueous phase concentrations of chemical compounds originating from particle scavenging, mass transfer from the gas phase and in-cloud aqueous chemical reactivity (Rose et al., 2018). A detailed description of this model is reported in SI-S5. This tool is specifically adapted for predicting the complexation and reactivity of Fe and organic ligands (siderophores and oxalate), which originate from the dissolution of activated aerosols. Table S2 presents the H_xO_y (sum of H_2O_2, •OH and HO_2•/O_2•$^-$) and Fe aqueous chemistry considered in the CLEPS model that is analysed hereafter. The concentrations and chemical budgets can be retrieved for all the gaseous and aqueous species described in the model. This model helps to discriminate the role of the various chemical and physical processes in the cloud system.

A gas phase spin-up simulation (7.5 days) was run to realistically initialize the gas phase concentrations before cloud formation (Table S3). The cloud simulation lasted 2 h (12 PM to 2 PM), and the physical conditions (notably the microphysical properties of the cloud) were kept constant. Summertime conditions were selected, with the simulation starting on June 1st, since it corresponds to optimal photolytic conditions and because 4 cloud events were collected during the summer period. Two distinct cloud simulations were performed: marine and continental scenarios that were carried out according to the average concentrations of ions detected at PUY for air masses of marine and continental origin (Renard et al., 2020). More details on the simulations are reported in SI-S5.

3. Results and discussion

3.1. Experimental determination of total Fe and Fe(III)-binding ligands in cloud water

The cloud water samples presented *TdFe* values ranging from 40 ± 6 nM to 323 ± 6 nM. The highest concentrations of total dissolved Fe (TdFe) were measured in continental clouds. The marine clouds had a mean value of 44 ± 4 nM, lower than that of continental clouds (178 ± 126 nM). *TdFe* levels had been previously measured at PUY and ranged from 100 to 910 nM, with consistently lower values in the marine origin clouds (Bianco et al., 2020). These concentrations are in the same or slightly higher range of previous studies: polluted clouds collected in China and Italy had *TdFe* concentrations ranging between 1 and 2.5 μM (Li et al., 2013; Liu et al., 2012; Cini et al., 2002), while continental clouds collected in Germany, Pakistan and Arizona, showed values slightly below 1 μM (Plessow et al., 2001; Fomba et al., 2015; Ghauri et al., 2001; Hutchings et al., 2009).

L_{Fe} concentrations ranged from 97 ± 22 nM to 430 ± 91 nM (Table 1 and Fig. 1). Only CW6 showed saturation of organic ligands with Fe, preventing any estimation of the L_{Fe} concentration and $K_{Cond,\ Fe^{3+}}$. The L_{Fe} levels in marine clouds were lower than those in continental clouds (Fig. 1). The ligands presented $\log K_{Cond,\ Fe^{3+}}$ values ranging from 21.3 ± 0.4 to 22.7 ± 0.1, causing all the samples to be ranked as L_1 or L_2-type ligands (Table 1). These results showed that 95.2–99.7% of Fe is complexed by organic ligands (Table 1) and suggest that, in contrast with the current estimation, Fe(III) is preferentially complexed by strong organic ligands such as siderophores ($\log K_{Cond,\ Fe^{3+}} > 21$) rather than by carboxylic acids such as oxalate ($\log K_{Cond,\ Fe^{3+}} < 10$). Siderophore-type compounds are typically produced by microorganisms for Fe acquisition in Fe-poor environments (Rue and Bruland, 1995; Witter et al., 2000; Butler, 1998; Mawji et al., 2011; Buck et al., 2010; Poorvin et al., 2011; Hider and Kong, 2010). Vinatier et al. (2016) showed that 42% of the 450 bacterial and yeast strains identified in cloud water were able to exude siderophores. These results are supported by the high abundance of γ-Proteobacteria in the marine cloud samples; these bacteria are the most active in siderophore production (Vinatier et al., 2016). Amato et al. showed the production of siderophores through a metatranscriptomic analysis of three cloud water samples (Amato et al., 2019). Our results highlight that the chemical and photochemical reactivities of Fe in the atmospheric aqueous phase have to be reconsidered due to the role of these binding ligands produced *in situ*.

The findings of this work are extremely important since Fe chemistry strongly impact cloud reactivity: Fe in cloud water is present as a complex with high stability constant, similar to the ones observed for siderophores and higher than the ones measured for oxalate and carboxylic acids. The complexation of Fe by siderophores makes it available for microbial metabolism in cloud water but also in other environments, after wet and dry deposition, casting new shadows on the understanding of Fe biogeochemical cycle. On the other hand, Fe reactivity is influenced by the presence of microorganisms, which have consequently a strong impact on its aqueous reactivity and therefore on cloud water oxidant capacity.

3.2. Modelling study of Fe speciation and its effect on cloud water oxidant capacity

To understand the effect of Fe complexation on cloud water oxidant capacity, we conducted a model study using CLEPS 1.1 (Mouchel-Vallon et al., 2017), using new developments reported in SI-S5 (Rose et al., 2018).

The concentrations of Fe were selected according to the experimental results of the marine and continental scenarios, as reported in Table 1. Fe was initialized as Fe(II), which was rapidly converted into Fe(III), and it reached equilibrium with the ligands (oxalate and L_{Fe}). This choice is supported by the fact that Fe(II) in clay minerals and in silicates is shown to be more soluble (Crusius et al., 2011) and soluble Fe is mostly present as Fe(II) in aerosol particles in both fine and coarse mode (Gao et al., 2019). Sensitivity tests performed with initialization of Fe as 1) 100% Fe(II), 2) 100% Fe(III) and 3) 50% Fe(II) and 50% Fe(III) show that the chemical equilibrium between species, governed by reactions 14–51 in Table S2, is reached after few seconds. The L_{Fe} concentrations were evaluated on the basis of the results shown in Table 1. Oxalate (Oxa) was initialized at 3 μM in agreement with the average concentration in the samples, without distinction between marine and continental scenarios, and was largely in excess compared to Fe and L_{Fe} concentrations.

Four different cases were simulated and analysed for the two chemical scenarios:

1- "No Oxa, No L_{Fe}": the initial concentrations of Oxa and L_{Fe} were set to 0.

2- "Oxa, No L_{Fe}": the initial concentration of Oxa was set to 3 μM, while the L_{Fe} concentration was set to 0.
3- "No Oxa, L_{Fe}": the initial concentration of Oxa was set to 0, while the L_{Fe} concentration was set as reported in Table S4.
4- "Oxa, L_{Fe}": the initial concentrations of Oxa and L_{Fe} were set as reported in Table S4.

These 8 simulations allowed us to evaluate the effect of the two ligands (Oxa and L_{Fe}) on Fe speciation. Two additional sensitivity tests were performed for the continental scenario, with the four different cases.

1- Sensitivity test 1 (ST1): Continental [Fe] × 2; compared to the continental case, the Fe concentration was doubled while the concentration of the L_{Fe} was kept constant.
2- Sensitivity test 2 (ST2): Continental [Fe] 1 μM [L_{Fe}] 1.77 μM (same Fe/L_{Fe} ratio as the continental case); the Fe concentration was higher and similar to those measured on continental sites (Fomba et al., 2015).

Sensitivity tests were performed to evaluate the speciation of Fe when its concentration was higher than the L_{Fe} concentration (ST1) and to assess the impact of Fe speciation on cloud reactivity (ST2). The continental scenario was chosen as a starting point for the sensitivity tests because continental air masses more frequently show high Fe concentrations than do marine air masses. A total of 16 simulations were thus performed and analysed (see Table S5 for summary).

We first evaluated the speciation of Fe in the aqueous phase. Fe is mainly found in 4 different forms in the CLEPS model: Fe(II) (as Fe^{2+}), Fe(III) (as Fe^{3+} and aqua-complexes $Fe(OH)^{2+}$ and $Fe(OH)_2^+$), Fe-Oxa ($Fe(C_2O_4)^+$, $Fe(C_2O_4)^{2-}$ and $Fe(C_2O_4)_3^{3-}$ and Fe-L. Two cases were initialized with Oxa (in the forms $H_2C_2O_4$, $HC_2O_4^-$, and $C_2O_4^{2-}$) concentrations equal to 0. However, Oxa is produced throughout the simulation by aqueous reactivity, reaching concentrations of 3 μM and 0.5 μM in the marine and continental scenarios, respectively (Fig. S2). Dismissing the chemistry of oxalate to stop its aqueous production would make the simulation unreliable, as it is too different from the reality. We decided to avoid modifying the chemistry of organic compounds in the model, considering the small impact of oxalate on Fe speciation and cloud oxidant capacity.

Fig. 2 depicts the relative concentrations (in percentage) of Fe(II), Fe(III), Fe-Oxa and Fe-L for each scenario and case. The values were extracted 1 h after cloud formation (at 1 PM). Fe speciation does not vary significantly during the cloud lifetime since the redox reactivity of Fe rapidly reaches equilibrium after a few minutes. In the presence of L_{Fe}, with and without Oxa, more than 95% of Fe is complexed with L_{Fe} and is stabilised in this form. There was an exception for the case in the continental ST1 (Fig. 2c), in which the Fe concentration was higher than the L_{Fe} concentration. On the other hand, when there is no L_{Fe}, the predominant form of Fe is Fe(II), even if the concentration of Oxa is more than 10 times greater than the concentration of Fe (marine case, Fig. 2a). This is due to the efficient photolysis of Fe-Oxa, which leads to Fe(II) (Table S2, R73 to R75).

Fe(III) was unstable at the considered pH (5.0 and 5.8 for continental and marine, respectively), and its concentration was very low, on the order of 10 nM for the continental case and 65 nM for ST2, always in the absence of L_{Fe}. Under the simulated conditions (daytime conditions and chemical scenarios), Fe(III) can only exist in cloud water complexed with strong organic ligands; otherwise, it is rapidly photo-reduced to Fe(II). The model results also showed that, in the absence of L_{Fe}, Fe(II) is more likely to be found than the Fe-Oxa complex. This is due to the photolysis

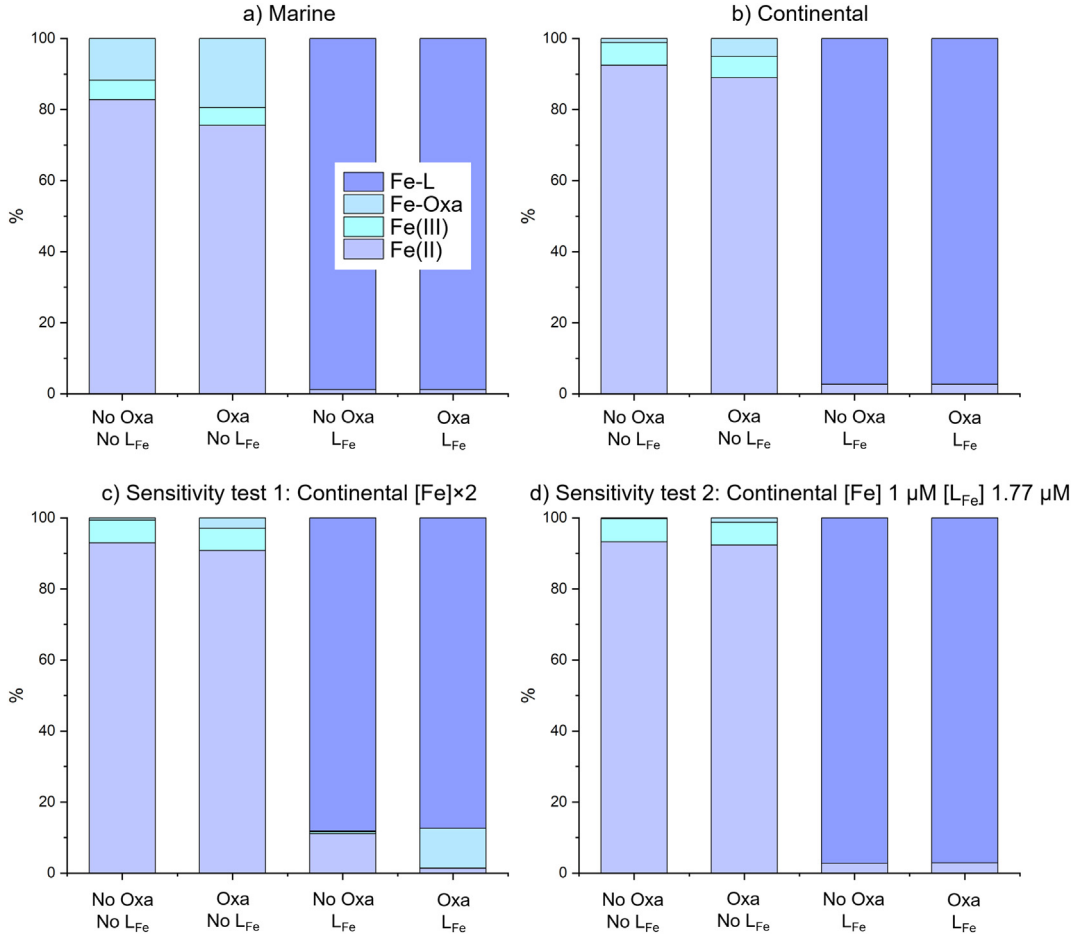

Fig. 2. Relative concentrations (in percentage) of Fe(II), Fe(III), Fe-Oxa and Fe-L for each scenario and case. The values are extracted 1 h after the cloud formation (at 1 PM).

of Fe-Oxa complexes that is considered in the model (Table S2), which leads to Fe(II) formation.

Fenton and Fe^{3+}-photolysis redox cycles, based on Fe chemistry, are crucial for the •OH formation rate (Deguillaume et al., 2005). The importance of these cycles naturally led us to investigate the impact of Fe complexation by L_{Fe} on cloud water oxidant capacity. At first glance, looking at the Fe redox cycle, we can expect that if Fe is free, it can react photochemically, and a higher concentration of •OH should be observed. Conversely, if Fe is complexed (Fe-L), we expect a lower concentration of •OH because it is not available for Fenton (Reaction R18, in Table S2) and photo-Fenton (Table S2, R15) redox cycles that are sources of •OH. Passananti et al. (2016) also determined the formation rate of Fe(II) for the irradiated complex at pH 4.0 and 6.0, finding values on the order of 10^{-9} M s^{-1}. The values were two orders of magnitude lower than those observed for the Fe-Oxa complex, confirming a stronger interaction between Fe and the organic ligand in the complex, which in this case was pyoverdine.

However, the oxidant capacity of cloud water is complex and implies the presence of other highly reactive species. Fe is directly involved in the Fenton reaction, with reaction with H_2O_2, or indirectly by reacting with peroxyl/superoxide radical anions (HO_2•/O_2•$^-$). Fig. 3 reports the concentrations of •OH and HO_2•/O_2•$^-$, whose equilibrium is governed by pH (pKa = 4.88). Surprisingly, the results for both marine and continental scenarios (Fig. 3a and b) show that the •OH concentrations are enhanced in the presence of L_{Fe}. At the end of the simulation, the •OH concentrations were 28% and 51% higher for the marine and continental cases respectively, in the presence of L_{Fe}. This difference was enhanced in ST1 (69%) as the •OH concentration more than doubled in ST2. This is because Fe is an important source of •OH, but it also efficiently consumes HO_2•/O_2•$^-$. When Fe is complexed by L_{Fe}, it cannot react with HO_2•/O_2•$^-$, which is a significant source of •OH through its reactivity with ozone (Table S2, R10–11). For continental and marine scenarios (Fig. 3a and b), the presence of ligands leads to an increase in the HO_2•/O_2•$^-$ concentrations. The same finding was observed for the continental case (Fig. 3b) based on ST1 and ST2 (Fig. 3c and d) sensitivity tests. At the end of the simulation, the difference in the HO_2•/O_2•$^-$ concentration varied between a 31% and 92% increase for the marine and continental scenarios, respectively. These differences were up to 2.7 and 7 times higher than the initial concentrations of ST1 and ST2, respectively. This result is of particular importance since highly variable •OH concentrations are simulated by cloud chemistry models, which demonstrates high degree of uncertainty in the •OH sources in the aqueous phase (Barth et al., 2021).

Sources and sinks of •OH can be analysed in detail. Fig. 4 depicts the sources of •OH for the marine scenario and for ST2. The cases "No Oxa, No L_{Fe}" (grey columns) and "No Oxa, L_{Fe}" (white columns) are taken into account. At first glance, the mass transfer (•OH radicals from the gas phase are transferred to the aqueous phase) and the reaction of ozone with HO_2• are the main sources of •OH in the aqueous phase (Table S2, R10 and R11), contributing 96–99% with and without L_{Fe}. The next sources in order of importance are H_2O_2 photolysis and the Fenton reaction, which can be considered negligible in the •OH chemical budget, with a contribution always lower than 5%. The H_2O_2 photolysis contribution can reach 3.7% of the •OH production rate in scenario ST2 without L_{Fe}, and the maximum for the Fenton reaction (4.2%) is reported for the same case and scenario. Fenton reaction is almost negligible because Fe is complexed by L_{Fe} and, consequently, the Fe(II) concentration is low. Fe complexation impacts the •OH formation rate through its crucial role in the reaction of ozone with HO_2•, which is much higher when Fe is complexed and cannot deplete HO_2•. We noticed an increase in the production rate of •OH by this reaction for ST2.

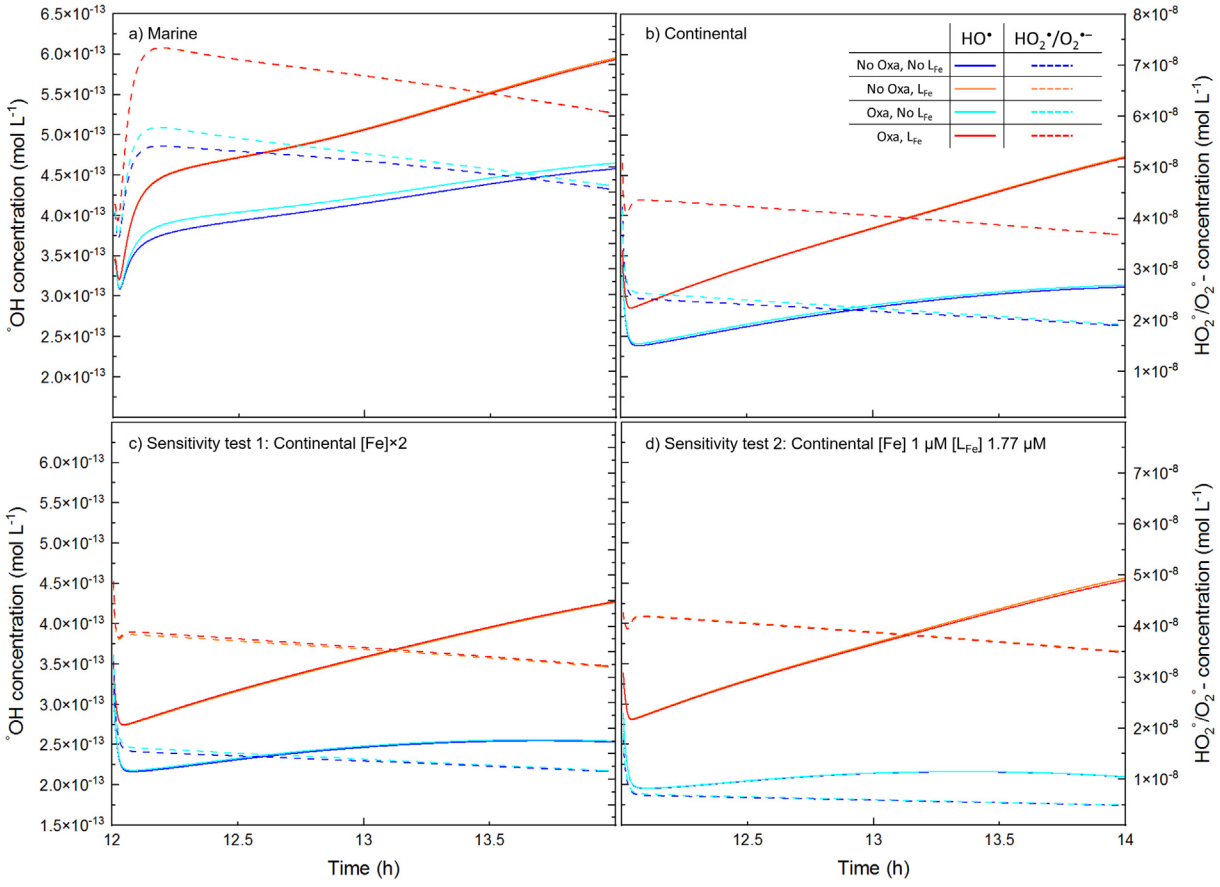

Fig. 3. Evolution with time of •OH concentration (mol L^{-1}), full line, and HO_2•/O_2•$^-$ concentration (mol L^{-1}), dashed line, for the four scenarios and four cases presented in this work. The legend is reported as insert in the plot b).

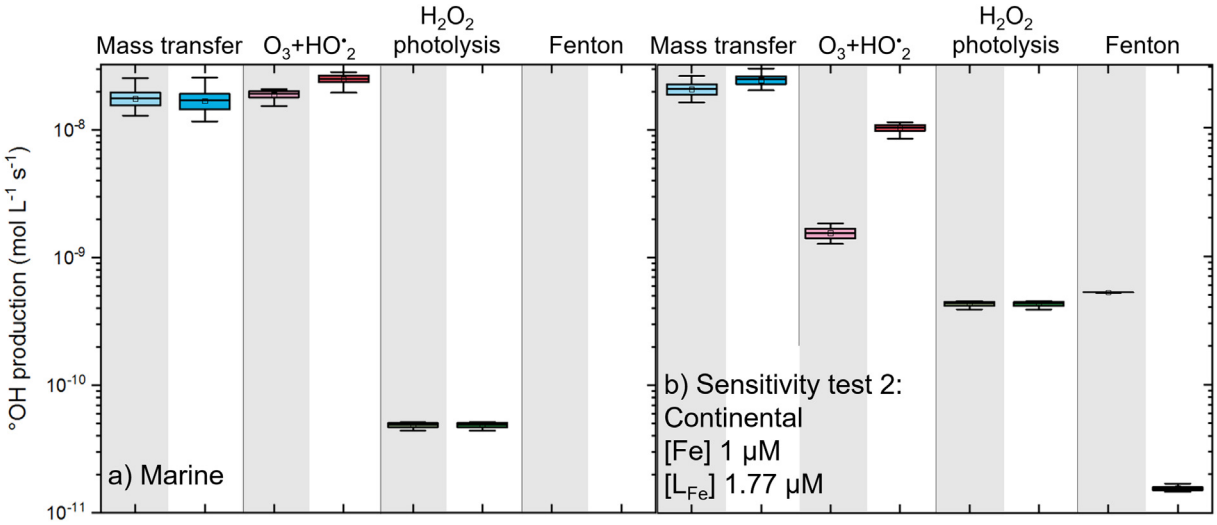

Fig. 4. Comparison of the sources of •OH for the case "No Oxa, No L_{Fe}", in grey, and "No Oxa, L_{Fe}", in white, for the marine scenario (a) and for the sensitivity test ST2 (b). Boxplots have been performed considering •OH production fluxes in the aqueous phase over the whole cloud period. Values below 10^{-11} mol L^{-1} s^{-1} are not reported in the plot and considered as negligible.

3.3. Atmospheric implications

The findings presented in this work lead to an important reconsideration of Fe chemistry and photochemistry in the atmospheric aqueous phase. Until now, Fe has been considered to be complexed by carboxylic acids, such as oxalate, or, in a few works, amino acids. Only recently, have researchers shown the potential production of siderophore compounds by microorganisms isolated from clouds and studied their photoreactivity (Passananti et al., 2016; Vinatier et al., 2016). Here, we present the first measurements of strong ligands, with binding constants comparable to those of siderophores, in cloud water, and we show that Fe is strongly complexed by organic ligands, which clearly affect its reactivity. Model results are in agreement with the experimental observations and confirm that more than 95% of Fe is complexed by strong organic ligands in clouds. Furthermore, the atmospheric deposition of Fe(III) as an organic complex may have a crucial impact on the bioavailability of Fe and should be considered in the assessment of its biogeochemical cycle. This result has a crucial implication: to survive in a harsh environment such as the atmosphere, microorganisms produce molecules to trap Fe, which consequently modify cloud water oxidant capacity. In this work we used CLEPS model to predict hydroxyl and peroxyl radical concentrations. To our knowledge, only few experimental studies evaluated the hydroxyl radical steady state concentrations in cloud waters: Lallement et al. (2018) and Anastasio and McGregor (2001) presented values of $7.2 \pm 5.0 \times 10^{-16}$ M and $7.2 \pm 5.0 \times 10^{-16}$ M, respectively, for some samples. These values are lower than the one predicted by CLEPS in this work but also lower than values predicted by other cloud chemistry models (Barth et al., 2021). This difference may be due to the absence of compounds with more than 4 carbon atoms in cloud chemistry models that can scavenge •OH. The environmental conditions (summertime) were also chosen to get optimal photochemical conditions for •OH production in the CLEPS model. Microbial metabolism has already been shown to be responsible for H_2O_2 depletion (Wirgot et al., 2017; Vaïtilingom et al., 2013), and the results presented in this work corroborate the need to consider microbial metabolism to better describe atmospheric chemistry.

CRediT authorship contribution statement

Conceptualization: L.D., A.-M.D., G.M., G.S.; Sampling: L.D., A.B.; Experimental measurements: A.B., M.C., J.B., H.P.; Statistical analysis: A.B.; Modelling: A.B., N.C., L.D.; Writing—original draft preparation: A.B., A.G.G.; Writing—review and editing; A.B., A.G.G., H.P., L.D., G.S., A.-M.D., G.M., M.C.; Funding: L.D., A.-M.D., G.M., G.S. All authors agreed with the submission of the manuscript. All authors have read and agreed to the published version of the manuscript.

Declaration of competing interest

The authors declare that they have no known competing financial interests or personal relationships that could have appeared to influence the work reported in this paper.

Acknowledgements

This work was supported by the project BIOCAP (ANR-13-BS06-0004). This work on the long-term analysis of the cloud water chemical composition was supported by the French Ministry and CNRS-INSU. Authors acknowledge additional financial support from the Observatoire de Physique du globe de Clermont-Ferrand (OPGC), from the Auvergne Regional Council, and from the Fédération des Recherches en Environnement through the CPER Environnement founded by Région Auvergne–Rhône-Alpes, the French ministry, and the FEDER from the European community. The authors also thank the I-Site CAP 20-25.

M. Vaïtilingom and M. Joly are gratefully acknowledged for helping in cloud sampling.

Appendix A. Supplementary data

Supplementary data to this article can be found online at https://doi.org/10.1016/j.scitotenv.2022.154642.

References

Aldrich, A.P., van den Berg, C.M.G., 1998. Determination of iron and its redox speciation in seawater using catalytic cathodic stripping voltammetry. Electroanalysis 10, 369–373.

Amato, P., et al., 2007. Microorganisms isolated from the water phase of tropospheric clouds at the puy de Dôme: major groups and growth abilities at low temperatures: microorganisms from the water phase of tropospheric clouds. FEMS Microbiol. Ecol. 59, 242–254.

Amato, P., et al., 2019. Metatranscriptomic exploration of microbial functioning in clouds. Sci. Rep. 9, 4383.

Anastasio, C., McGregor, K.G., 2001. Chemistry of fog waters in California's Central Valley: 1. In situ photoformation of hydroxyl radical and singlet molecular oxygen. Atmos. Environ. 35 (6), 1079–1089.

Baray, J.-L., et al., 2020. Cézeaux-aulnat-opme-puy De Dôme: a multi-site for the long-term survey of the tropospheric composition and climate change. Atmos. Meas. Tech. 13, 3413–3445.
Barth, M.C., et al., 2021. Box model intercomparison of cloud chemistry. J. Geophys. Res. Atmos. 126, e2021JD035486.
Bianco, A., et al., 2015. A better understanding of hydroxyl radical photochemical sources in cloud waters collected at the puy de Dôme station – experimental versus modelled formation rates. Atmos. Chem. Phys. 15, 9191–9202.
Bianco, A., Passananti, M., Brigante, M., Mailhot, G., 2020. Photochemistry of the cloud aqueous phase: a review. Molecules 25, 423.
Buck, K.N., Selph, K.E., Barbeau, K.A., 2010. Iron-binding ligand production and copper speciation in an incubation experiment of Antarctic Peninsula shelf waters from the Bransfield Strait, Southern Ocean. Mar. Chem. 122, 148–159.
Buesseler, K.O., et al., 2008. Environment: ocean iron fertilization-moving forward in a sea of uncertainty. Science 319 162-162.
Butler, A., 1998. Acquisition and utilization of transition metal ions by marine organisms. Science 281, 207–209.
Cheize, M., et al., 2012. Iron organic speciation determination in rainwater using cathodic stripping voltammetry. Anal. Chim. Acta 736, 45–54.
Cini, R., et al., 2002. Chemical characterization of cloud episodes at a ridge site in Tuscan Appennines, Italy. Atmos. Res. 61, 311–334.
Crusius, J., et al., 2011. Glacial flour dust storms in the Gulf of Alaska: hydrologic and meteorological controls and their importance as a source of bioavailable iron. Geophys. Res. Lett. 38, L06602.
Deguillaume, L., et al., 2005. Transition metals in atmospheric liquid phases: sources, reactivity, and sensitive parameters. Chem. Rev. 105, 3388–3431.
Deguillaume, L., et al., 2014. Classification of clouds sampled at the puy de Dôme (France) based on 10 yr of monitoring of their physicochemical properties. Atmos. Chem. Phys. 14, 1485–1506.
Deutsch, F., Hoffmann, P., Ortner, H., 2001. Field experimental investigations on the fe (II)- and fe (III)-content in cloud water samples. J. Atmos. Chem. 40, 87–105.
Fomba, K.W., et al., 2015. Trace metal characterization of aerosol particles and cloud water during HCCT 2010. Atmos. Chem. Phys. 15, 8751–8765.
Gao, Y., et al., 2019. Particle-size variability of aerosol iron and impact on iron solubility and dry deposition fluxes to the Arctic Ocean. Sci. Rep. 9, 16653.
Ghauri, B.M., et al., 2001. Composition of aerosols and cloud water at a remote mountain site (2.8 kms) in Pakistan. Chemosphere Global Change Sci. 3, 51–63.
Gledhill, M., Buck, K., 2012. The organic complexation of iron in the marine environment: a review. Front. Microbiol. 3, 69.
Gledhill, M., Buck, K.N., 2012. The organic complexation of iron in the marine environment: a review. Front. Microbiol. 3, 1–17.
González, A.G., Cadena-Aizaga, M.I., Sarthou, G., González-Dávila, M., Santana-Casiano, J.M., 2019. Iron complexation by phenolic ligands in seawater. Chem. Geol. 511, 380–388.
Herckes, P., Valsaraj, K.T., Collett, J.L., 2013. A review of observations of organic matter in fogs and clouds: origin, processing and fate. Atmos. Res. 132–133, 434–449.
Herrmann, H., 2003. Kinetics of aqueous phase reactions relevant for atmospheric chemistry. Chem. Rev. 103, 4691–4716.
Herrmann, H., et al., 2015. Tropospheric aqueous-phase chemistry: kinetics, mechanisms, and its coupling to a changing gas phase. Chem. Rev. 115, 4259–4334.
Hider, R.C., Kong, X., 2010. Chemistry and biology of siderophores. Nat. Prod. Rep. 27, 637.
Huang, W., Brigante, M., Wu, F., Hanna, K., Mailhot, G., 2012. Development of a new homogenous photo-Fenton process using Fe(III)-EDDS complexes. J. Photochem. Photobiol. A Chem. 239, 17–23.
Hutchings, J.W., Robinson, M.S., McIlwraith, H., Triplett Kingston, J., Herckes, P., 2009. The chemistry of intercepted clouds in northern Arizona during the north american monsoon season. Water Air Soil Pollut. 199, 191–202.
Johnson, M.S., Meskhidze, N., 2013. Atmospheric dissolved iron deposition to the global oceans: effects of oxalate-promoted fe dissolution, photochemical redox cycling, and dust mineralogy. Geosci. Model Dev. 6, 1137–1155.
Lallement, A., et al., 2018. First evaluation of the effect of microorganisms on steady state hydroxyl radical concentrations in atmospheric waters. Chemosphere 212, 715–722.
Li, W., et al., 2013. Microscopic evaluation of trace metals in cloud droplets in an acid precipitation region. Environ. Sci. Technol. 47, 4172–4180.
Liu, X., Millero, F.J., 2002. The solubility of iron in seawater. Mar. Chem. 77, 43–54.
Liu, X., et al., 2012. Evaluation of trace elements contamination in cloud/fog water at an elevated mountain site in northern China. Chemosphere 88, 531–541.
Luther, G.W., Rozan, T.F., Witter, A., Lewis, B., 2001. Metal–organic complexation in the marine environment. Geochem. Trans. 2, 65.
Mawji, E., et al., 2011. Production of siderophore type chelates in Atlantic Ocean waters enriched with different carbon and nitrogen sources. Mar. Chem. 124, 90–99.
Mouchel-Vallon, C., et al., 2017. CLEPS 1.0: a new protocol for cloud aqueous phase oxidation of VOC mechanisms. Geosci. Model Dev. 10, 1339–1362.
Nagai, T., Imai, A., Matsushige, K., Yokoi, K., Fukushima, T., 2007. Dissolved iron and its speciation in a shallow eutrophic lake and its inflowing rivers. Water Res. 41, 775–784.
Passananti, M., Vinatier, V., Delort, A.-M., Mailhot, G., Brigante, M., 2016. Siderophores in cloud waters and potential impact on atmospheric chemistry: photoreactivity of iron complexes under sun-simulated conditions. Environ. Sci. Technol. 50, 9324–9332.
Plessow, K., Acker, K., Heinrichs, H., Möller, D., 2001. Time study of trace elements and major ions during two cloud events at the Mt. Brocken. Atmos. Environ. 35, 367–378.
Poorvin, L., et al., 2011. A comparison of fe bioavailability and binding of a catecholate siderophore with virus-mediated lysates from the marine bacterium vibrio alginolyticus PWH3a. J. Exp. Mar. Biol. Ecol. 399, 43–47.
Renard, P., et al., 2020. Classification of clouds sampled at the puy de Dôme Station (France) based on chemical measurements and air mass history matrices. Atmosphere 11, 732.
Rose, C., et al., 2018. Modeling the partitioning of organic chemical species in cloud phases with CLEPS (1.1). Atmos. Chem. Phys. 18, 2225–2242.
Rue, E.L., Bruland, K.W., 1995. Complexation of iron (III) by natural organic ligands in the central North Pacific as determined by a new competitive ligand equilibration/adsorptive cathodic stripping voltammetric method. Mar. Chem. 50, 117–138.
Sherman, D.M., 2005. Electronic structures of iron(III) and manganese(IV) (hydr)oxide minerals: thermodynamics of photochemical reductive dissolution in aquatic environments. Geochim. Cosmochim. Acta 69, 3249–3255.
Sigg, L., Behra, P., Stumm, W., 2001. Chimie des milieux aquatiques. Dunod.
Skidmore, M.L., Foght, J.M., Sharp, M.J., 2000. Microbial life beneath a high Arctic glacier. Appl. Environ. Microbiol. 66, 3214–3220.
Tapparo, A., et al., 2020. Formation of metal-organic ligand complexes affects solubility of metals in airborne particles at an urban site in the Po valley. Chemosphere 241, 125025.
Toom-Sauntry, D., Barrie, L.A., 2002. Chemical composition of snowfall in the high Arctic: 1990–1994. Atmos. Environ. 36, 2683–2693.
Vaïtilingom, M., et al., 2013. Potential impact of microbial activity on the oxidant capacity and organic carbon budget in clouds. Proc. Natl. Acad. Sci. 110, 559–564.
Vinatier, V., et al., 2016. Siderophores in cloud waters and potential impact on atmospheric chemistry: production by microorganisms isolated at the puy de Dôme Station. Environ. Sci. Technol. 50, 9315–9323.
Warneck, P., 2000. Chemistry of the Natural Atmosphere. Academic Press.
Willey, J.D., et al., 2000. Temporal variability of iron speciation in coastal rainwater. J. Atmos. Chem. 37, 185–205.
Wirgot, N., Vinatier, V., Deguillaume, L., Sancelme, M., Delort, A.-M., 2017. H2O2 modulates the energetic metabolism of the cloud microbiome. Atmos. Chem. Phys. 17, 14841–14851.
Witter, A.E., Hutchins, D.A., Butler, A., Luther, G.W., 2000. Determination of conditional stability constants and kinetic constants for strong model fe-binding ligands in seawater. Mar. Chem. 69, 1–17.